Photoacoustic microscopy with an enhanced axial resolution of 5.8 μm

Chi Zhang, Yong Zhou, Chiye Li, Lihong V. Wang

Chi Zhang, Yong Zhou, Chiye Li, Lihong V. Wang, "Photoacoustic microscopy with an enhanced axial resolution of 5.8 μm," Proc. SPIE 8943, Photons Plus Ultrasound: Imaging and Sensing 2014, 894316 (3 March 2014); doi: 10.1117/12.2036832

SPIE.

Event: SPIE BiOS, 2014, San Francisco, California, United States

Photoacoustic microscopy with an enhanced axial resolution of 5.8 μm

Chi Zhang, Yong Zhou, Chiye Li, and Lihong V. Wang*
Department of Biomedical Engineering, Washington University in St. Louis, One Brookings Drive, St. Louis, MO 63130, USA
* Corresponding author: LHWANG@WUSTL.EDU

ABSTRACT

The axial resolution of photoacoustic microscopy (PAM) can be enhanced by reducing the speed of sound within the imaging region of interest. This principle was demonstrated on a previously-reported PAM system, which utilized a 125 MHz ultrasonic transducer for signal detection and the Wiener deconvolution for signal processing. With sound slowed by silicone oil immersion, we have achieved a finest axial resolution of 5.8 μm for PAM, as validated by phantom experiments. The axial resolution was also enhanced *in vivo* when mouse ears injected with silicone oil were imaged. After injection of silicone oil, the blood vessels were resolved more clearly. When tissue-compatible low-speed liquids become available, this approach may find applications in PAM as well as in other imaging modalities, such as photoacoustic computed tomography and ultrasound imaging.

Keywords: photoacoustic microscopy, axial resolution, speed of sound

1. INTRODUCTION

Photoacoustic microscopy (PAM) is a three-dimensional (3D) imaging technology capable of imaging optical absorption of biomolecules with a relative sensitivity of 100% [1]. Label-free PAM has demonstrated broad biomedical applications by imaging hemoglobin, melanin, DNA & RNA in nuclei, cytochromes, lipids, bilirubin, etc. [2-7] over an optical wavelength range from middle-UV to near-infrared. In typical PAM, the optical absorbers are irradiated by a laser pulse, and then the excited photoacoustic wave is detected by an ultrasonic transducer. In optical-resolution PAM, the lateral resolution is determined by the spot size of the optical focus, and the axial resolution is normally determined by the width of the temporal impulse response of the PAM system. While submicron lateral resolution has been achieved for PAM [8, 9], the finest axial resolution still remains on the micron level [10, 11], much poorer than the lateral resolution.

If the impulse response of the PAM system is assumed to have a Gaussian envelope, the axial resolution of PAM can be estimated as $0.88\,c\,/\,B$, where c is the speed of sound and B is the bandwidth of the PAM system. To enhance the axial resolution, broad bandwidth B has been realized by using a very broadband ultrasonic transducer [10] or optical resonance acoustic sensor [11]. However, the penetration depth of PAM decreases with the bandwidth because the acoustic attenuation increases with the frequency. On the other hand, optically-determined axial resolution can be achieved for PAM by using nonlinear optical effects [12], such as in two-photon-absorption PAM [13]. Although promising, this technique is expected to have relatively low detection sensitivity, and its 3D image acquisition time is lengthened by the additional depth scanning.

For the first time, we propose to enhance the axial resolution of PAM by reducing the speed of sound c. If we consider two objects separated by a given spatial distance, the time interval between the two objects is inversely proportional to the speed of sound between them. Since an ultrasonic transducer detects the time-resolved signal, reducing the speed of sound would shorten the smallest resolvable distance between objects. Note that here the time interval is determined by the speed of sound of the medium between them, while the speed of sound of the medium between the objects and the ultrasonic transducer determines the "time delay" of both signals from the two objects. Therefore, in our method, we aim to reduce the speed of sound inside the imaging region of interest instead of in the surrounding coupling medium (typically water or ultrasonic gel).

To reduce the speed of sound inside the imaging region of interest, we can either immerse the sample in a liquid that has a relatively low speed of sound, or inject the liquid into the sample. With a lower speed of sound, the immersion liquid is expected to have a different acoustic impedance Z ($= \rho c$, where ρ is the density) from that of the surrounding medium. The acoustic wave will be reflected at the interface in the case of acoustic impedance mismatch. Hence, the acoustic

Photons Plus Ultrasound: Imaging and Sensing 2014, edited by Alexander A. Oraevsky, Lihong V. Wang,
Proc. of SPIE Vol. 8943, 894316 · © 2014 SPIE · CCC code: 1605-7422/14/$18 · doi: 10.1117/12.2036832

impedance mismatch will decrease the detected signal amplitude and generate reverberation. In most biomedical applications of PAM, the acoustic impedances of the imaged soft tissues and the coupling water are about 1.6 MRayl and 1.5 MRayl, respectively, while the speeds of sound are approximately 1.5×10^3 m/s.

To demonstrate the principle of our method, here we choose silicone oil (85421, Sigma-Aldrich) as the immersion liquid, whose speed of sound is about 1.1×10^3 m/s and acoustic impedance is about 1.1 MRayl. With silicone oil immersion, we can estimate that the axial resolution will be enhanced by ~1.4 times. The acoustic impedance mismatch introduced by silicone oil is relatively low, as the amplitude reflection coefficient between the silicone oil and water is 0.16. Moreover, silicone oil is non-toxic and has been used in medical applications, such as in eye injection for managing complicated retinal detachments [14, 15] and in soft tissue injection for tissue augmentation [16, 17]. Therefore, silicone oil is a relatively simple and safe choice for injection into biological tissues to reduce the speed of sound.

2. MATERIALS AND METHODS

The experimental PAM system is shown in Fig. 1 [18]. Laser pulses were generated by a tunable OPO laser (NT242-SH, Ekspla) with 5 ns pulse width, 1 KHz pulse repetition rate, and 532 nm wavelength. The laser pulses were spatially filtered by a 50 μm pinhole and then focused by a 0.32 NA objective, providing ~0.8 μm lateral resolution. Photoacoustic waves were excited by the focused laser pulse irradiating the sample. The imaging region of interest of the sample was immersed in silicone oil. The photoacoustic waves were detected by an ultrasonic transducer (125 MHz central frequency, 100 MHz bandwidth; V2062, Olympus NDT), which was immersed in water for coupling. The photoacoustic signals were amplified and digitized at 1 GS/s (PCI-5152, National Instruments). The sample was mounted on a scanning stage (PLS-85, MICOS). Both the laser and the scanning stage were triggered by a homemade controller, and the data acquisition card was triggered by the laser output for synchronization. Each time-resolved photoacoustic signal was converted to a 1D depth-resolved image by the Wiener deconvolution method, and the sample was mechanically scanned in 2D to generate a 3D image.

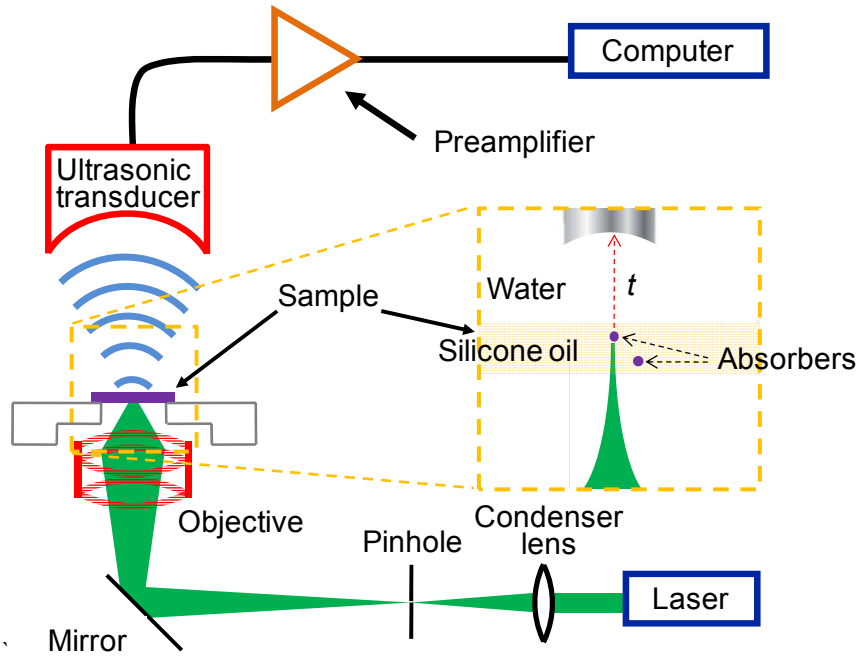

Figure 1. System schematic of PAM.

3. RESULTS AND DISCUSSION

We designed an experiment to quantitatively measure the axial resolution of the PAM system. Shown in Fig. 2(a), the sample to be imaged consists of two layers of red ink, the upper one on polymethylpentene (TPX) plastic and the lower one on a glass slide. The two layers were placed in a wedge shape, providing continuously variable distance between the two layers. The top layer was smeared on the TPX plastic because the acoustic impedance of TPX is close to that of water. The gap between the two layers was filled with either water or silicone oil for comparison, and the space between the two layers and the ultrasonic transducer was filled with water for coupling. B-scan images of the water-filled sample and the silicone-oil-filled sample are shown in Figs. 2(b) and 2(c), respectively. In both images, the vertical direction is plotted in the units of time. It can be seen that the bottom layer of ink, which was placed horizontally, appears oblique in Fig. 2(c). The reason is that as the thickness of the silicone oil in the gap increases, the photoacoustic signal from the bottom layer takes longer to travel to the ultrasonic transducer due to the slower speed of sound in silicone oil than in water. For the same reason, the two layers can be separated more clearly. The axial resolution is defined as the distance with 6 dB contrast-to-noise ratio (CNR). It can be calculated that the axial resolution of the PAM system is 7.8 μm with water immersion, and is 5.8 μm with silicone oil immersion. Figures 2(d) and 2(e) show the profiles across the B-scan images with water and silicone oil immersion, respectively, where the axial resolution is defined with 6 dB CNR.

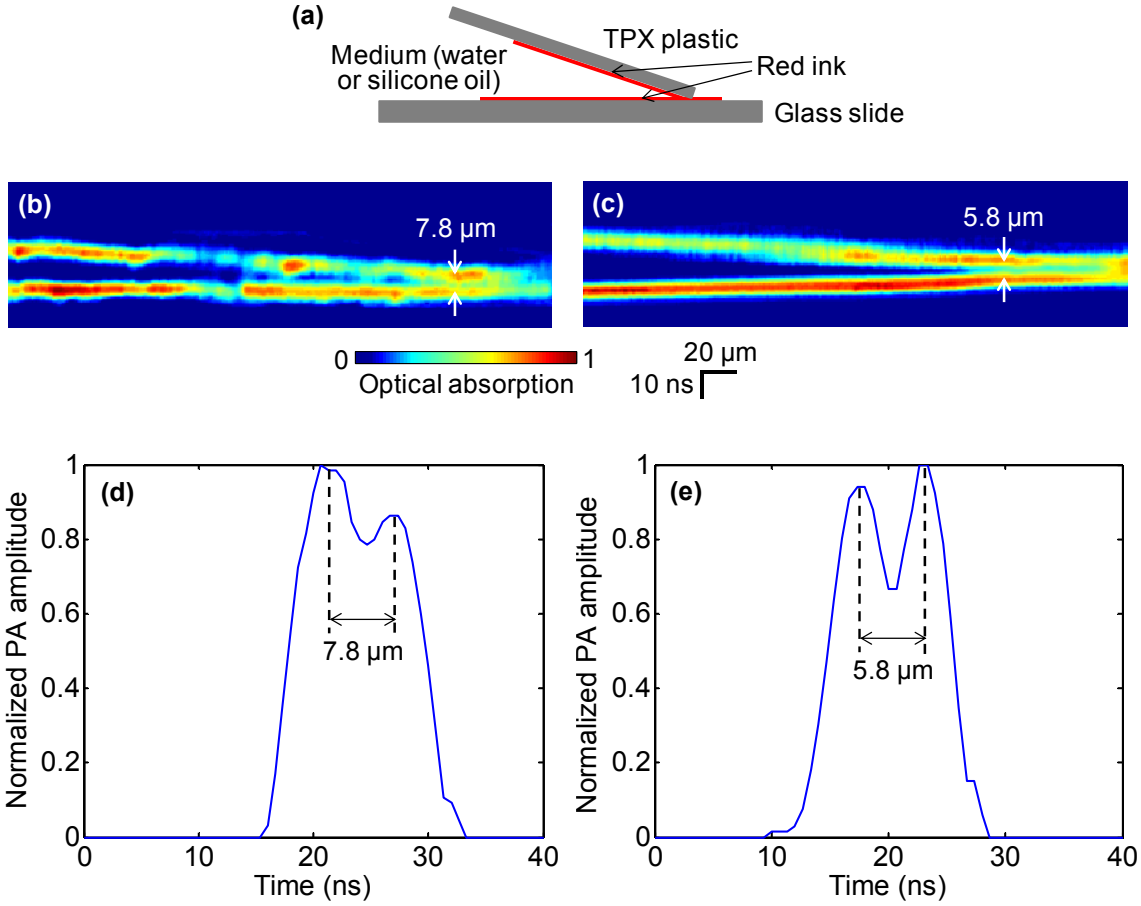

Figure 2. (a) The sample to be imaged consists of two layers of red ink in a wedge shape. (b) B-scan image of the sample with water immersion. (c) B-scan image of the sample with silicone oil immersion. (d) Profile across the B-scan image where the distance between the two layers is 7.8 μm. (e) Profile across the B-scan image where the distance between the two layers is 5.8 μm.

We used the high-axial-resolution PAM system to image melanoma cells *ex vivo*. The cells were seeded onto a slide at a density of 30 cells per mm^{-2} and fixed by formalin. The PAM image of a melanoma cell is rendered in 3D as a video (Video 3). The bright dots in the PAM images are melanosomes, the organelles containing melanin. The 3D structure of the cell was resolved in both lateral and axial directions. Note that here PAM generates a 3D image without depth scanning, which, however, is required in confocal microscopy and two photon microscopy.

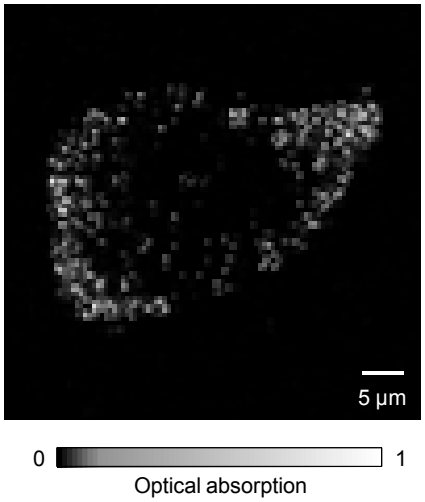

Video 3. 3D PAM image of a melanoma cell *ex vivo*. http://dx.doi.org/10.1117/12.2036832.1

We also showed potential biomedical applications of our method. We injected silicone oil into a mouse ear to enhance the axial resolution *in vivo*. Approximately 30 μL of silicone oil was injected into a nude mouse ear and allowed to diffuse for 30 min. Top view mouse ear images, before and 30 min after silicone oil injection, are shown in Figs. 4(a) and 4(b), respectively. The area was imaged with the same laser intensity before and after the injection. The top-view images, as shown in Figs. 4(a) and 4(b), are very similar. However, the side-view images of the same area demonstrate the improvement in axial resolution achieved by injecting silicone oil, as shown in Figs. 4(c) and 4(d). To show the improvement in axial resolution more clearly, the amplitudes along the dashed profiles in Figs. 4(c) and 4(d) are shown in Figs. 4(e) and 4(f), respectively. The two major blood vessels are resolved more clearly with silicone oil injection.

It is possible to further improve the axial resolution, at the cost of detection sensitivity, by using an immersion liquid with a lower speed of sound, such as fluorosilicone oil (7.6×10^2 m/s) or tallow (3.9×10^2 m/s). Theoretically, tallow can help achieve an axial resolution of 2.0 μm for non-biological samples. For biomedical applications, we will seek more low-speed biocompatible immersion liquids.

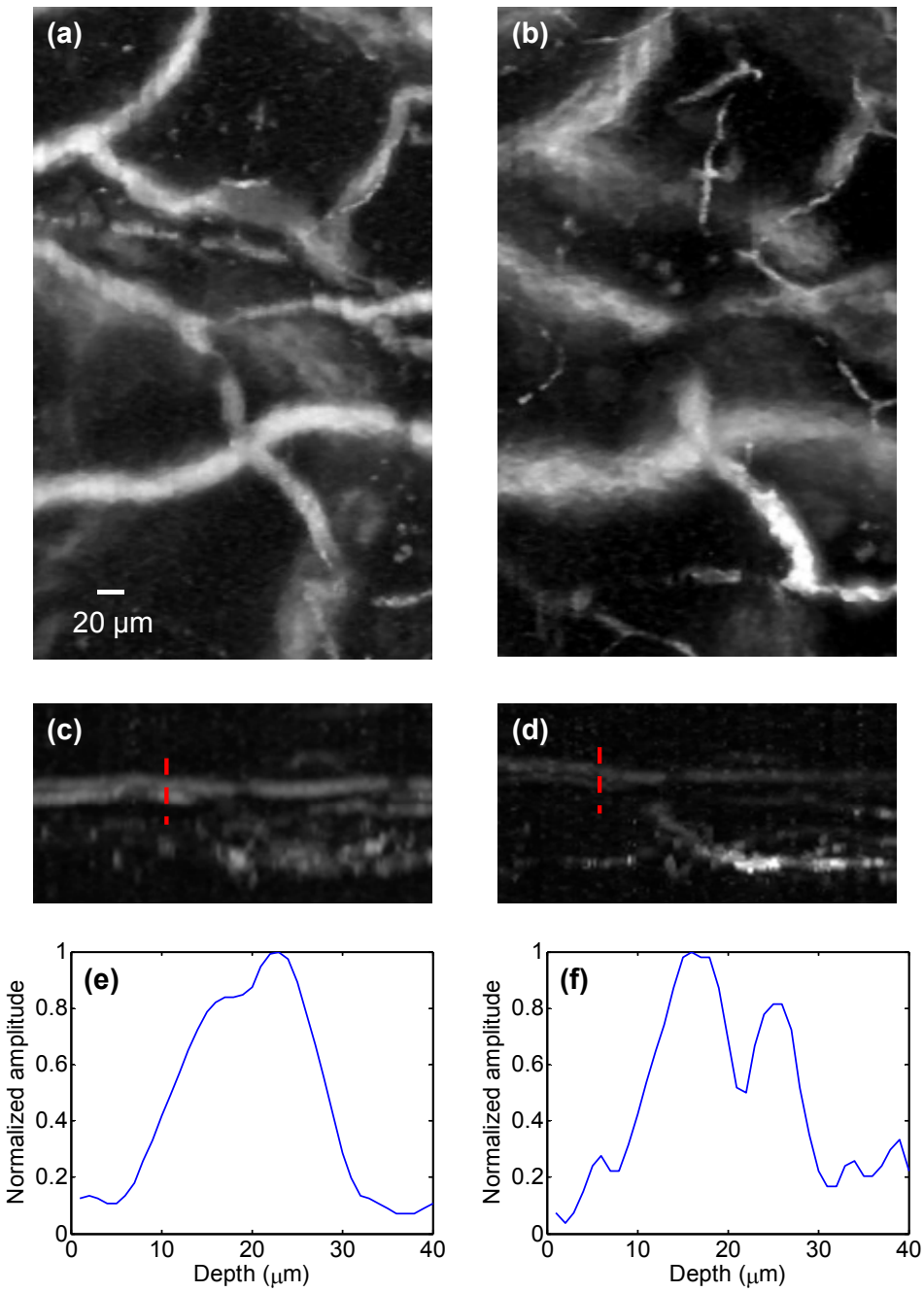

Figure 4. *In vivo* top-view PAM images of a mouse ear before (a) and after (b) injection of silicone oil. Side-view PAM images before (c) and after (d) injection of silicone oil. (e) Normalized PA amplitude along the dashed line in (c). (f) Normalized PA amplitude along the dashed line in (d).

4. CONCLUSIONS

We have demonstrated that the axial resolution of PAM can be enhanced by using an immersion liquid to reduce the speed of sound. With silicone oil immersion, we achieved a finest axial resolution of 5.8 μm. We also improved the axial resolution in imaging mouse ears *in vivo* after silicone oil injection. Our method can potentially be applied to cell

imaging [19, 20] and be used in other imaging modalities, such as photoacoustic computed tomography and ultrasound imaging.

ACKNOWLEDGMENT

This work was sponsored in part by National Institutes of Health grants DP1 EB016986 (NIH Director's Pioneer Award), R01 CA134539, U54 CA136398, R01 CA157277, and R01 CA159959. L.W. has a financial interest in Microphotoacoustics, Inc. and Endra, Inc., which, however, did not support this work.

REFERENCES

[1] L. V. Wang, and S. Hu, "Photoacoustic Tomography: In Vivo Imaging from Organelles to Organs," Science, 335(6075), 1458-1462 (2012).

[2] H. F. Zhang, K. Maslov, G. Stoica *et al.*, "Functional photoacoustic microscopy for high-resolution and noninvasive in vivo imaging," Nat. Biotechnol., 24(7), 848-51 (2006).

[3] D.-K. Yao, K. Maslov, K. K. Shung *et al.*, "In vivo label-free photoacoustic microscopy of cell nuclei by excitation of DNA and RNA," Optics Letters, 35(24), 4139-4141 (2010).

[4] C. Zhang, Y. S. Zhang, D.-K. Yao *et al.*, "Label-free photoacoustic microscopy of cytochromes," Journal of Biomedical Optics, 18(2), 020504-020504 (2013).

[5] H.-W. Wang, N. Chai, P. Wang *et al.*, "Label-Free Bond-Selective Imaging by Listening to Vibrationally Excited Molecules," Physical Review Letters, 106(23), 238106 (2011).

[6] Y. Zhou, C. Zhang, D.-K. Yao *et al.*, "Photoacoustic microscopy of bilirubin in tissue phantoms," Journal of Biomedical Optics, 17(12), 126019-126019 (2012).

[7] T. P. Matthews, C. Zhang, D.-K. Yao *et al.*, "Label-free photoacoustic microscopy of peripheral nerves," Journal of biomedical optics, 19(1), 016004-016004 (2014).

[8] C. Zhang, K. Maslov, and L. V. Wang, "Subwavelength-resolution label-free photoacoustic microscopy of optical absorption in vivo," Opt. Lett., 35(19), 3195-3197 (2010).

[9] C. Zhang, K. Maslov, S. Hu *et al.*, "Reflection-mode submicron-resolution in vivo photoacoustic microscopy," Journal of Biomedical Optics, 17(2), 020501-1 (2012).

[10] C. Zhang, K. Maslov, J. Yao *et al.*, "In vivo photoacoustic microscopy with 7.6-μm axial resolution using a commercial 125-MHz ultrasonic transducer," Journal of Biomedical Optics, 17(11), 116016-116016 (2012).

[11] Z. Xie, S.-L. Chen, T. Ling *et al.*, "Pure optical photoacoustic microscopy," Optics express, 19(10), 9027 (2011).

[12] J. Yao, L. Wang, C. Li *et al.*, "Photoimprint Photoacoustic Microscopy for Three-Dimensional Label-Free Subdiffraction Imaging," Physical Review Letters, 112(1), 014302 (2014).

[13] Y. Yamaoka, M. Nambu, and T. Takamatsu, "Fine depth resolution of two-photon absorption-induced photoacoustic microscopy using low-frequency bandpass filtering," Opt. Express, 19(14), 13365-13377 (2011).

[14] J. Federman, and H. D. Schubert, "Complications associated with the use of silicone oil in 150 eyes after retina-vitreous surgery," Ophthalmology, 95(7), 870-876 (1988).

[15] D. Tognetto, D. Minutola, G. Sanguinetti *et al.*, "Anatomical and functional outcomes after heavy silicone oil tamponade in vitreoretinal surgery for complicated retinal detachment: a pilot study," Ophthalmology, 112(9), 1574. e1-1574. e8 (2005).

[16] R. J. Rohrich, and J. K. Potter, "Liquid Injectable Silicone:: Is There a Role as a Cosmetic Soft-Tissue Filler?," Plastic and reconstructive surgery, 113(4), 1239-1241 (2004).

[17] P. E. Chasan, "The history of injectable silicone fluids for soft-tissue augmentation," Plastic and reconstructive surgery, 120(7), 2034-2040 (2007).

[18] C. Zhang, Y. Zhou, C. Li *et al.*, "Slow-sound photoacoustic microscopy," Applied Physics Letters, 102(16), 163702 (2013).

[19] L. Gao, C. Zhang, C. Li *et al.*, "Intracellular temperature mapping with fluorescence-assisted photoacoustic-thermometry," Applied Physics Letters, 102(19), 193705-193705-5 (2013).

[20] C. Li, C. Zhang, L. Gao *et al.*, "Photoacoustic recovery after photothermal bleaching in living cells," Journal of biomedical optics, 18(10), 106004-106004 (2013).